

BEAM INSTRUMENTATION FOR CRYRING@ESR

A. Reiter*, C. Andre, H. Bräuning, C. Dorn, P. Forck, R. Haseitl, T. Hoffmann, W. Kaufmann, N. Kotovski, P. Kowina, K. Lang, R. Lonsing, P. Miedzik, T. Milosic, A. Petit, H. Reeg, C. Schmidt, M. Schwickert, T. Sieber, R. Singh, G. Vorobjev, B. Walasek-Höhne, M. Witthaus
 GSI Helmholtz-Centre for Heavy Ion Research GmbH, Darmstadt, Germany

Abstract

The beam instrumentation of the CRYRING@ESR experimental storage ring is described. As part of the future FAIR facility, all systems are being developed to be compliant with the new software and hardware standards. The current status is presented as commissioning continues throughout 2018.

THE CRYRING@ESR PROJECT

CRYRING@ESR, together with experimental storage ring (ESR) and HITRAP decelerator, provide new opportunities for research fields with highly-charged ions (HCI) at low energies [1–4]. Apart from injection of a $\sim 3 \mu\text{s}$ long bunch of cooled HCI from ESR, multi-turn injection from a radiofrequency-quadrupole linac (RFQ) delivers light ions. Beam optics and injection schemes are described in [5].

The linac was commissioned in 2016 [3] and used during the long shutdown of the GSI facility since autumn of that year. Beam storage was achieved in August 2017 [6], followed by cooling attempts in November when the electron cooler came online. In March 2018, Ar⁺ and Mg⁺ ions were injected at 40 kV ion source potential (operating the RFQ in transport mode), accelerated and stored for lifetime measurements in preparation of experiments at the end of the year. H₂⁺ beams were accelerated to full rigidity of 1.4 Tm. Commissioning will resume in August.

The former CRYRING synchrotron and storage ring, operated originally at Manne-Siegbahn laboratory in Stockholm, has been moved to GSI in 2013 as Swedish in-kind contribution to the FAIR facility [7,8]. It since has been reassembled behind ESR, thus giving birth to its new name. The machine has undergone a substantial technical overhaul which included a full replacement of all beam instrumentation data acquisition systems (DAQ) [9], while most of the existing detector hardware remained unchanged. Modified layout and instrumentation are shown in Fig. 1 and summarised in Table 1. As first FAIR machine and in its function as test bench, the facility is founded on new standards and technologies, most importantly the general machine timing system based on White Rabbit [10], parameter settings management LSA [11], the front-end software architecture (FESA) framework for data acquisition systems [12], and new control and calibration hardware for ring cavities [13, 14].

BEAM INSTRUMENTATION

The beam instrumentation is discussed after some general remarks on commissioning conditions. The compact

* a.reiter@gsi.de

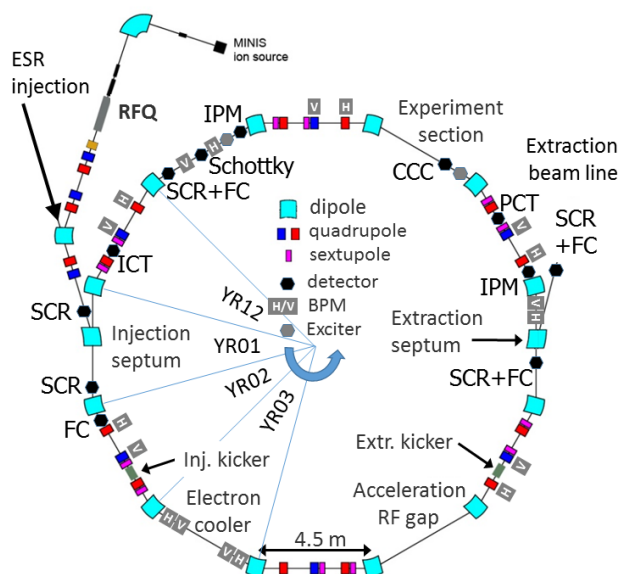


Figure 1: ESR and RFQ injections, and detector positions in storage ring and extraction beam line as listed in Table 1.

RFQ linac provided mainly singly-charged H₂⁺ beams [3]. The 1.6 m long structure operates at 108.48 MHz and can accelerate beams of charge-to-mass ratio (q/A) ≥ 0.35 from 10 to 300 keV/u [15, 16]. Currents exceeded 30 μA regularly, in some cases with full transmission. Details on the linac diagnostics can be found in [17].

For multi-turn injection a 50 μs pulse was chosen, during machine setup often shortened to 4–5 μs beamlets (< 1 turn). At 54.18 m circumference and 300 keV/u energy, a single revolution took 7.2 μs ($f_{rev} \sim 140$ kHz). Prior to rf capture in 4–9 s long machine cycles, DC currents of 10 μA (4.5×10^8 charges) and more were stored. A mean vacuum pressure of 1×10^{-11} mbar allowed lifetimes of several seconds.

1st Turn Diagnostics

The 1st turn is closed with Faraday cups (FC) and scintillation screens (SCR). At the end of injection section YR01 a Cromox screen with remote-controlled iris and focus is mounted on a stepper motor drive. It replaces a beam position monitor (BPM) because of the ~ 50 mm offset between the two injection schemes. All other detectors are mounted on pneumatic drives. The injected current is optimised behind the first dipole with a FC in section YR02. Further diagnostics chambers in sections YR07 and YR11 are equipped with a 65 mm FC and a 100 mm P43 phosphor screen.

Digital 10 bit CMOS cameras record images in triggered or free-run mode. Cameras and lens systems are controlled by an industrial PC which hosts the CUPID software for

Content from this work may be used under the terms of the CC BY 3.0 licence (© 2018). Any distribution of this work must maintain attribution to the author(s), title of the work, publisher, and DOI.

Table 1: Beam Instrumentation by Ring Section

Section	Detector	Task
Injection line	SCR (Cromox)	profile before injection septum
YR01	SCR (Cromox)	profile after septum and el.-stat. bumper
YR02	FC BPM (h+v)	injection efficiency position
YR03	BPM (h+v) BPM (v+h)	positions in electron cooler
YR06	BPM (h+v)	position
YR07	SCR (P43) + FC BPM (h+v)	1st turn diagnostics position
YR08	Hor. IPM BPM (h+v) Bergoz PCT	profile, intensity position DC current
YR09	Hor. exciter Cryogenic Current Comparator (CCC)	tune, beam transfer function (BTF) current
YR10	BPM (h+v)	position
YR11	Vert. IPM Vert. exciter Schottky detector BPM (h+v) SCR (P43) + FC	profile, intensity tune, BTF intensity, tune, etc. position 1st turn diagnostics
YR12	BPM (h+v) Bergoz ICT	position, intensity AC current, charge

analogue and digital imaging [18]. To avoid excessive light yields the pulse length is cut to one or two turns. Figure 2 presents a beam spot at the end of section YR01. Once the first turn is closed, the multi-turn injection scans the "up-right" distribution horizontally through a decreasing local orbit bump to fill the synchrotron acceptance.

Beam Position and Orbit

The beam position monitors (BPM) are 150 mm long, diagonally-cut cylinders which offer good position linearity. In the "even", magnetic sections YR02, YR06,..., YR12 they are installed in the first two quadrupoles. The "uneven" sections host special installations, and BPMs are installed where possible. Some were sacrificed to make room for experiment hardware. This causes the irregular distribution along the ring, see Fig. 1 or Table 1. Their standard diameter is 100 mm, while four smaller units of 77 mm are fitted in the cooler section YR03, two at each end. These BPMs have a larger capacitance of ~100 pF compared to 40 pF of the standard BPMs. New high-impedance amplifiers feature 40 or 60 dB gain, input protection, and the option to reduce the bandwidth from 40 MHz to 4 MHz. After signal transmis-

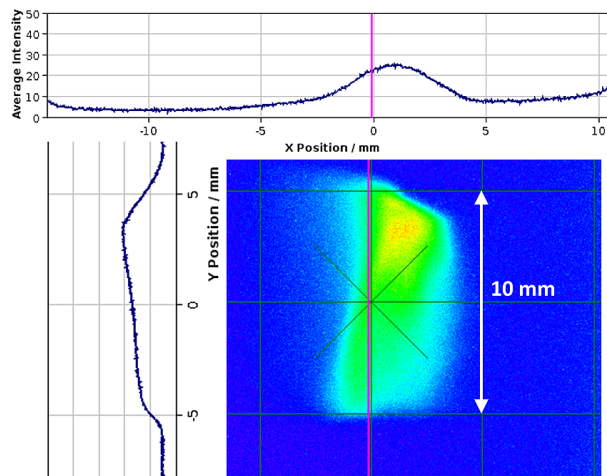


Figure 2: Beam profiles at end of injection section YR01. The horizontal and vertical histograms are projections of the two-dimensional camera image in the region of interest.

sion, active or passive splitters provide dedicated sum and diagnostic signals. So far, especially at low currents, the good signal quality has proven to be very beneficial.

The DAQ is an open-hardware design based on the modern μ TCA standard [19]. Signals are acquired by 125 MSa/s ADCs with 16 bit resolution. Positions are evaluated online on the FPGA from the slope of a straight-line least-squares fit [20] in user-defined or turn-by-turn sample block sizes. The position data stream is then reduced in rate by a configurable averaging stage, e.g. to 1 or 10 kHz. A first prototype system is expected to be operational by mid-2018. Currently, a simple DAQ acquires a 100 μ s snapshot (15 turns) of signal traces, positions and orbit of a user-defined 20 ms interval within the cycle, and a 1 s long storage of all raw data.

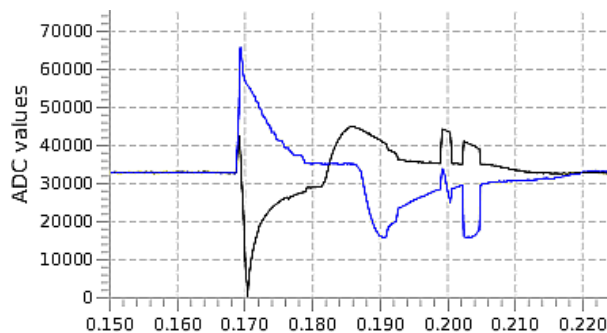


Figure 3: BPM signals at injection of a 5 μ s macropulse in a 75 μ s window. Large positive and negative signals indicate a direct hit on or near an electrode.

During injection and the first turns the BPMs act as beam loss detectors, and the DAQ displays all raw data traces in a 100 μ s interval. When the primary beam hits an electrode, a large positive signal is generated, while the secondary electrons ejected from its surface travel towards the opposite electrode and cause negative cross talk. One example which covers the full ADC input range is presented in Fig. 3 for the first BPM in the electron cooler. Later much smaller signals (~5% of ADC range) are recorded after rf capture when

bunches of parabolic shape have developed with a length close to the 7 μ s revolution period. Correlating these data with DC transformer currents, one can estimate the detection limit for such a pulse to be about 1×10^7 charges.

Dipole ripple was estimated from 50-turn horizontal position data that showed variations between 0.3 and 1 mm depending on BPM location. These relate to a current ripple of $\sim 2 \times 10^{-5}$ with respect to 120 A at injection plateau. This value is in line with the power supply specification. The three strongest contributions in the frequency spectra are even harmonics at 100, 200 and 300 Hz. Another line at 266 Hz is caused by the operating frequency of a control DAC in the dipole power supply [21]. These lines are consistent in all BPM data, while the BPMs in cooler section YR03 show additional noise below 100 Hz and a strong 70 kHz line induced by the 7 kV supplies of the ion getter pumps.

Some data sets have revealed larger oscillations of up to 5 mm with a broad frequency distribution below 500 Hz. Preliminary tests pointed to the power supply's harmonic filter, but must be continued to be fully conclusive.

Ionisation Profile Monitors

For profile measurements two ionisation profile monitors (IPM) are available, one for each transverse plane [22, 23]. Note that at RFQ energy the electric field of 45 kV/m deflects the beam by several mrad. Each IPM detects vertices of ionisation events with a Chevron-type MCP stack and a position-sensitive resistive anode encoder. The charge-sensitive pre-amplifier signals are shaped in a spectroscopy amplifier, and the output signals analysed by a peak-sensing ADC in a VME system. The FESA class on the controller converts the four anode signal amplitudes to a vertex and fills online histograms at a maximum rate of ~ 20 kHz. The profiles of Fig. 4 were constructed from a raw data file exported in parallel. The achievable resolution of 0.3 mm FWHM is yet to be confirmed, e.g. with cooled ESR beams.

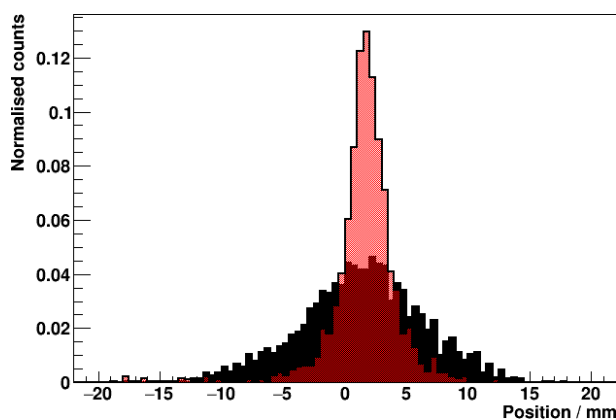


Figure 4: Vertical profiles measured with 0.5 mm resolution at the start of the cooling (black) and after 5 seconds (red).

Current and Beam Intensity

All hardware has been described in [24–26]. Here, we briefly comment on ongoing activities and modifications. The aim remains the ability to track beam currents down to

the nA level, while currents of up to 50 μ A can be expected by ESR injection. A pilot beam time in 2016 had transported $\sim 5 \times 10^7$ C^{6+} ions of 12 MeV/u towards CRYRING@ESR.

Data acquisition The VME scaler system LASSIE [27] replaces the ADC system and records all intensity signals, but also the main magnets, at a standard rate of 1 kHz.

DC transformer A two-layer mu-metal shield should be ready for installation before the August run in order to suppress stray fields of surrounding magnets. During machine cycles without beam, transformer distortions were recorded separately for six magnets and repeated for various excitation levels. The target is a remaining distortion $< 1 \mu$ A in order to avoid the need for further compensation measures, e.g. in software or via compensation loops.

Dual-Integrator The signal synchronisation between integration gate, derived from gap rf master signal and a dedicated CEL calibration unit [13, 14], and the two input signals of AC transformer and BPM sum was tested, but not to maximum frequency and only at low beam intensity.

CryRadio The most sensitive device is the frequency mixer unit fed by a second BPM sum signal. Its 10.7 MHz output carrier is now processed in a logarithmic amplifier with demodulator to access the amplitude information. A voltage-to-frequency converter then feeds the scaler readout.

Cryogenic Current Comparator For absolute measurements in the nA region a new UHV-compatible CCC design with 150 mm aperture is under construction and ready for installation in experiment section YR09 by the end of this year [28, 29].

Schottky Detector and Exciter

In the solenoid section YR11, horizontal and vertical pairs of 1380 mm long and 50 mm high Schottky electrodes are installed. At a separation of 100 mm their capacitance is ~ 130 pF. Low-noise 50 dB Trontec W50ATC amplifiers are directly mounted on the upstream ports. For comparison the performance of high-impedance amplifiers will be evaluated next. Sum and difference signals are derived in a hybrid combiner unit and fed to a spectrum analyser (SA) and a real-time SA via a remote-controlled switching matrix.

For tune and beam transfer function, a horizontal or vertical exciter generates a maximum electrode voltage of 100 V within a bandwidth of 3 MHz. The electrode length is 75 mm, their separation 60 mm. The exciter output is gated via a programmable external trigger pulse.

The FESA class development will start when the new hardware setup has been finalised.

ACKNOWLEDGEMENTS

The authors are grateful to numerous colleagues of GSI accelerator division and CRYRING@ESR community for their fruitful collaboration throughout the project and ongoing commissioning campaigns.

REFERENCES

- [1] M. Lestinsky *et al.*, CRYRING@ESR Study Group Report, June 2012, www.fair-center.eu/for-users/publications/experiment-collaboration-publications.html
- [2] M. Lestinsky *et al.*, "Physics book: CRYRING@ESR", *Eur. Phys. J. Special Topics* 225, 797–882 (2016).
- [3] Geithner, W., Andelkovic, Z., Beck, D. *et al.*, "Status and outlook of the CRYRING@ESR project", *Hyperfine Interact* (2017) 238: 13. DOI: 10.1007/s10751-016-1383-5
- [4] F. Herfurth *et al.*, "The HITRAP facility for slow highly charged ions", 2015 *Phys. Scr.* **2015** 014065.
- [5] O. Gorda *et al.*, "Ion optics of CRYRING@ESR", *Phys. Scr.* T166 (2015) 014043.
- [6] F. Herfurth *et al.*, "Commissioning of the low energy storage ring facility CRYRING@ESR", in *Proc. of COOL'17*, Bonn, Germany, DOI: 10.18429/JACoW-COOL2017-THM13, 2018.
- [7] FAIR baseline technical report, vol. 1–6, 2006, <https://fair-center.eu/for-users/publications/fair-publications.html>
- [8] FAIR Green Paper - The Modularized Start Version, October 2009, <https://fair-center.eu/for-users/publications/fair-publications.html>
- [9] T. Hoffmann *et al.*, "Beam Instrumentation and Data Acquisition for CRYRING@ESR", in *Proc. ICALEPCS'15*, Melbourne, Australia, paper MOPGF022, pp.133–136.
- [10] D. Beck *et al.*, "The new White Rabbit based timing system for the FAIR facility", in *Proc. PCaPAC'12*, Kolkata, India, paper FR1A01, pp. 242–244.
- [11] D. Jacquet, R. Gorbonosov, G. Kruk, and P.P. Mira, "LSA – the high level application software of the LHC and its performance during the first 3 years of operation", in *Proc. ICALEPCS'13*, San Francisco, CA, USA, paper THPPC058, pp. 1201–1204.
- [12] M. Arruat *et al.*, "Front-End Software Architecture", in *Proc. of ICALEPCS'07*, Knoxville, Tennessee, USA, paper WOPA04, pp. 310–312.
- [13] S. Schäfer, H. Klingbeil, B. Zipfel, A. Klaus and U. Hartel, "Use of FPGA-based configurable electronics to calibrate cavities", in *Proc. IPAC'13*, Shanghai, China, paper THPEA003, pp. 3152–3154.
- [14] B. Zipfel *et al.*, "Generation of rf frequency and phase references on the FAIR site", in *Proc. IPAC'14*, Dresden, Germany, DOI: 10.18429/JACoW-IPAC2014-THPR0102, 2014.
- [15] A. Schempp *et al.*, "The CRYRING RFQ for heavy ion acceleration", in *Proc. of EPAC'90*, pp.1231–1233.
- [16] A. Schempp *et al.*, "RFQ-Injector for CRYRING", in *Proc. of EPAC'88*, pp. 590–592.
- [17] A. Reiter *et al.*, "Beam instrumentation of the RFQ injector at CRYRING", GSI Scientific Report 2016, DOI: 10.15120/GSI-2017-00527, p. 405.
- [18] B. Walasek-Höhne *et al.*, "CUPID: New System for Scintillating Screen Based Diagnostics", in *Proc. of IBIC'14*, Monterey, CA, USA, TUPD006, pp. 417–420.
- [19] P. B. Miedzik, H. Bräuning, T. Hoffmann, A. Reiter, and R. Singh, "A MicroTCA based Beam Position Monitoring System at CRYRING@ESR", in *Proc. of ICALEPCS'17*, Barcelona, Spain, DOI: 10.18429/JACoW-ICALEPCS2017-TUPHA075, 2018.
- [20] A. Reiter and R. Singh, "Comparison of beam position calculation methods for application in digital acquisition systems", *NIM A* 890 (2018), pp. 18–27.
- [21] D. Novak *et al.*, "Scraping the CRYRING beam - a simple diagnostic tool", *Nucl. Phys.* A626 (1997), 511c-514c.
- [22] A. Källberg, A. Paal, J. Gal, J. Molnar and G. Szekely, "NIM-PC based read-out electronics for residual-gas ionization beam profile monitors at the CRYRING", in *Proc. of DIPAC'97*, Frascati (Rome), Italy, pp. 150–152.
- [23] A. Reiter, H. Bräuning, T. Milosic, H. Reeg and T. Sieber, "Beam Profile Measurements and Observation of Beam Cooling at CRYRING@ESR", GSI scientific report 2017.
- [24] A. Paal, A. Simonsson and A. Källberg, "Current measurement of low-intensity beams at CRYRING", in *Proc. of DIPAC'03*, Mainz, Germany, paper PT28, pp. 240–241.
- [25] A. Paal, A. Simonsson, A. Källberg, J. Dietrich and I. Mohos, "Methods and instrumentation for measurement of low ion beam currents at CRYRING", in *Proc. of EPAC'04*, Lucerne, Switzerland, paper THPLT112, pp. 2748–2749.
- [26] A. Paal, A. Simonsson, J. Dietrich and I. Mohos, "Bunched beam current measurements with 100 pA RMS resolution at CRYRING", in *Proc. of EPAC'06*, Edinburgh, Scotland, paper TUPCH080, pp. 1196–1198.
- [27] T. Hoffmann, H. Bräuning and R. Haseitl, in *Proc. of ICALEPCS'11*, Grenoble, France, paper MOPMN008, pp. 250–252.
- [28] T. Sieber *et al.*, "Optimization of the Cryogenic Current Comparator (CCC) for Beam Intensity Measurement", in *Proc. of IBIC'17*, Michigan, USA, DOI: 10.18429/JACoW-IBIC2017-TH2AB3, 2018.
- [29] P. Seidel *et al.*, "Cryogenic Current Comparators for Larger Beamlines", in *IEEE Transactions on Applied Superconductivity*, vol. 28, no. 4, pp. 1–5, June 2018.